Electrocatalytically Active Graphene–Platinum Nanocomposites. Role of 2-D Carbon Support in PEM Fuel Cells

ARTICLE *in* THE JOURNAL OF PHYSICAL CHEMISTRY C · MAY 2009

Impact Factor: 4.77 · DOI: 10.1021/jp900360k

2 AUTHORS:

Brian Seger
Technical University of Denmark
40 PUBLICATIONS **2,998** CITATIONS

SEE PROFILE

Prashant Kamat
University of Notre Dame
539 PUBLICATIONS **44,417** CITATIONS

SEE PROFILE

THE JOURNAL OF PHYSICAL CHEMISTRY C LETTERS

2009, *113,* 7990–7995
Published on Web 04/15/2009

Electrocatalytically Active Graphene-Platinum Nanocomposites. Role of 2-D Carbon Support in PEM Fuel Cells

Brian Seger and Prashant V. Kamat*

Radiation Laboratory, Departments of Chemistry & Biochemistry and Chemical & Biomolecular Engineering, University of Notre Dame, Notre Dame, Indiana 46556-0579

Received: January 13, 2009; Revised Manuscript Received: March 27, 2009

The use of a 2-D carbon nanostructure, graphene, as a support material for the dispersion of Pt nanoparticles provides new ways to develop advanced electrocatalyst materials for fuel cells. Platinum nanoparticles are deposited onto graphene sheets by means of borohydride reduction of H_2PtCl_6 in a graphene oxide (GO) suspension. The partially reduced GO-Pt catalyst is deposited as films onto glassy carbon and carbon Toray paper by drop cast or electrophoretic deposition methods. Nearly 80% enhancement in the electrochemically active surface area (ECSA) can be achieved by exposing partially reduced GO-Pt films with hydrazine followed by heat treatment (300 °C, 8 h). The electrocatalyst performance as evaluated from the hydrogen fuel cell demonstrates the role of graphene as an effective support material in the development of an electrocatalyst.

Introduction

Carbon supported electrocatalysts are effective in maximizing the performance of proton exchange membrane (PEM) based fuel cells and minimizing the use of precious metals, typically Pt.[1] Such support materials not only maximize the availability of nanosized electrocatalyst surface area for electron transfer but also provide better mass transport of reactants to the electrocatalyst. In addition, the conductive support facilitates efficient collection and transfer of electrons to the collecting electrode surface. Carbon black, because of its high surface area, high conductivity, and low cost, has been extensively used as a support for PEM based solar cells.

Recently many different carbon based materials such as single walled nanotubes,[2] multiwalled nanotubes,[3] stacked nanocups,[4] and graphitic nanofibers,[5] have been used as electrocatalyst supports in fuel cells. The goal is to utilize these carbon nanostructures as highly conductive carbon scaffolds to attain large surface areas on which to disperse platinum nanoparticles. Other nanostructured materials with large surface areas and high conductivity have also been tested as supports for dispersing electrocatalysts.[6−8] One issue that calls for new and improved carbon materials is the long-term stability of carbon supports under fuel cell operation.[9] Durability tests have indicated that conventional carbon black supports undergo morphological changes and induce catalyst aggregation during extended use.[10] Carbon nanotubes have shown better stability than carbon black.[10]

The recent emergence of graphene nanoelectronics has opened a new avenue for utilizing 2-dimensional carbon material as a support in PEM fuel cells.[11] One hopes to employ such 2-D sheets as conductive mats to both anchor electrocatalysts and modulate the electrochemical reactions in a controlled fashion (Scheme 1). Graphene is a single sheet of sp^2 hybridized carbon

SCHEME 1: Dispersion of Pt Nanoparticles on a 2-D Carbon Sheet (Graphene) to Facilitate an Electrocatalytic Reaction

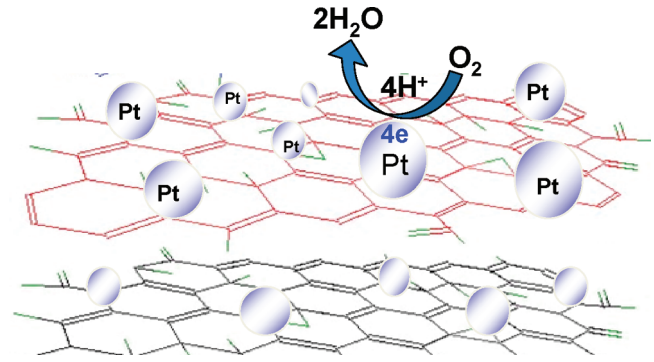

that can be exfoliated from bulk graphite using mechanical cleavage,[12] thermal exfoliation,[13] and chemical functionalization.[14,15] Though the chemical oxidation method is convenient to exfoliate graphene sheets via solution based processes, it introduces functional groups such as carboxyl and epoxides.[16] The presence of these functional groups makes the individual graphene oxide sheets suspendable in both polar and nonpolar solvents but drastically decreases the conductivity as a result of a loss in the conjugated sp^2 network. Hydrazine has been widely used to reduce graphene oxide and increase the conductivity[17] by restoring the sp^2 hybridized network. Other reductants such as $NaBH_4$ and hydroquinone have also been found useful.[17,18] Recently we showed that graphene oxide can be reduced via a TiO_2 assisted photocatalytic method.[19] The deposition of TiO_2 nanoparticles assisted in dispersing graphene oxide sheets in solution.

The graphene sheets serve as a stabilizer in the synthesis of silver and gold nanoparticles. The particle size can be controlled by varying the graphene oxide ratio.[20,21] Graphene sheets have also been found to be useful in anchoring semiconductor

* Author to whom correspondence should be addressed. E-mail: pkamat@nd.edu.

10.1021/jp900360k CCC: $40.75

particles such as TiO_2.[19] The ability of graphene sheets to support nanoparticles opens new ways to develop electrocatalysts for fuel cells. We now report here the deposition of Pt nanoparticles on reduced graphene oxide sheets and their utilization in proton exchange membrane assembly. The characterization of the Pt-graphene composite and the evaluation of electrocatalytic performance presented in this study provide an insight into the utilization of a graphene as a 2-D carbon support in fuel cells.

Experimental Section

Materials. Graphite, H_2PtCl_6, $NaBH_4$ and $N_2H_4-H_2O$ were obtained from Alfa-Aeser, while $KMnO_4$ and $NaNO_3$ were obtained from Mallinckrodt (St. Louis, Missouri). H_2SO_4, HCl, and 30% H_2O_2 were all obtained from Fischer Scientific. Nafion ionomer was obtained from Ion Power; Nafion 115 and carbon Toray paper were obtained from ElectroChem (Woburn, MA); and the gas diffusion layers (GDL LT 1200-N) were obtained from Fuelcellstore.com. Vulcan XC-72 carbon black was obtained from Cabot.

Graphite was oxidized to graphene oxide (GO) using the Hummers method.[15] In brief, this method consists of stirring graphite powder (Aldrich) in a solution with strong oxidizing agents such as potassium permanganate and concentrated sulfuric acid. The oxidation needs to be carried out in a hood and protective gear worn during the entire process. The mixture is then neutralized and subjected to several cycles of centrifugation and washing with deionized water. The dried powder is stored and dispersed in solvents as needed.

Synthesis of GO-Pt Particles. Graphene oxide was mixed with H_2PtCl_6 in an aqueous solution. The ratio of graphene oxide to platinum in this mixture was 1:1 by mass. HCl was then added until the pH was <2, and the solution was stirred for at least 30 min. A 50 mM solution of $NaBH_4$ solution was added dropwise until all the H_2PtCl_6 was reduced to metallic platinum. This solution was centrifuged and washed 3 times in 0.1 M HCl. Known amounts of Nafion ionomer were added to the solid. The material was then suspended in either water or tetrahydrofuran. Before any deposition of the GO-Pt as a film on an electrode surface, the solution was sonicated for at least 30 min. For comparison, pure platinum and a 1:1 ratio of carbon black to platinum were used as supports for depositing Pt via reduction of H_2PtCl_6. In these cases the suspension was not acidified and the reduction was carried out under the natural pH of the solution.

Electrode Preparation. Three different methodologies were adopted to prepare GO-Pt electrodes. In the first method, 20 μL of GO-Pt suspension containing 1 mg/L Pt and 1 mg/L GO was drop cast onto a glassy carbon electrode. The concentration of platinum in these electrodes was determined by atomic emission spectroscopy using an Inductively Coupled Plasma (ICP) spectrometer. In the second method, a tetrahydrofuran solution containing GO-Pt was deposited dropwise onto a 1 cm^2 of carbon Toray paper to attain a concentration of $\sim$10 μg Pt/cm^2. The third method consisted of GO-Pt in a tetrahydrofuran solution being electrophoretically deposited (EPD) onto 1 cm^2 area of carbon Toray paper (4 cm $\times$ 0.5 cm size) at 75 V/cm. The deposition conditions were adjusted such that a concentration of $\sim$10 μg/cm^2 Pt was achieved. The details of the EPD process can be found elsewhere.[6,22] Unless otherwise stated all values in the figures have been normalized to a constant Pt amount of 1 mg/cm^2.

Membrane Electrode Assembly (MEA) Preparation. Gas diffusion layers were purchased from Electrochem and cut into 5 cm^2 electrodes. The anode was sprayed with 0.5 mg/cm^2 Pt of an E-Tek CB-Pt (40% Pt on CB (with 30% Nafion)) catalyst. This high loading allowed us to eliminate overpotential issues on the anode and, therefore, allowed us to focus solely on the cathode.[23] The Pt loading of each cathode was 0.2 mg/cm^2 with 30% Nafion by weight. Nafion 115 was used as the proton exchange membrane. The details of the pretreatment of the Nafion as well as the MEA hot press procedure are given in our previous work.[8]

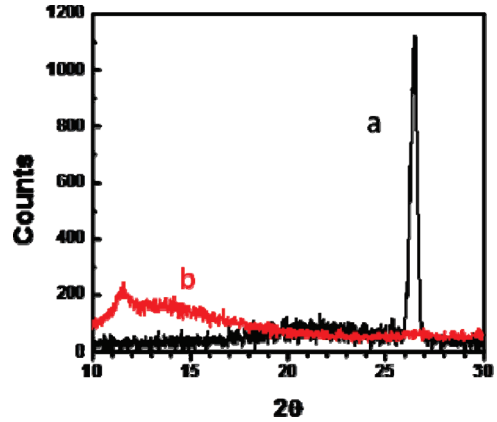

Figure 1. XRD diffraction data of graphite samples (a) before and (b) after oxidation. The shift from a sharp peak at 26.5° to a broad peak near 12° shows functionalization of the graphene sheets.

Methods. A Metler-Toledo TGA/SDTA851e TGA analysis machine was used to analyze the graphene oxide and Nafion ionomer (1100 EW). The temperature went from 25 to 600 °C at a rate of 10 °C per minute. Atomic force microscopy (AFM) images of the GO-Pt on a mica sheet (2 cm $\times$ 2 cm size) were obtained using a digital Nanoscope IIIa Atomic Force Microscope. Characterization of the surface was carried out in the tapping mode with silicon tips (Nanoprobe Tapping Mode TAP 300, TESP). All electrochemical studies were carried out using a Gamry Framework Version 4.35. A 3-electrode cell consisting of the catalyst as the working electrode, platinum as the counter and a saturated calomel electrode (SCE) as a reference electrode was used in all cases.

A single cell test fixture supplied by Electrochem Inc. was employed for evaluating the catalyst performance for H_2/O_2 based fuel cell. The MEA was inserted between two graphite plates, which had a serpentine flow pattern. Two Teflon gaskets of thickness 0.24 mm were introduced between the membrane and electrodes. A uniform torque of 35 in.-pounds was applied to each of the bolts used to assemble the cell. The fuel cell was connected to the test station (Scribner Associates, Inc., USA), which was equipped with a gas humidifier, a mass flow controller, and a temperature indicator controller. Humidified hydrogen and oxygen gases were fed into the cell at a flow rate of 200 cm^3 min^{-1} and 400 cm^3 min^{-1} respectively, and the cell temperature maintained at 60 °C. The current−voltage ($I-V$) characteristics of the cell were then evaluated.

Results and Discussion

Graphene Oxide. As described in the experimental section graphene oxide was prepared by the chemical oxidation of commercially obtained graphite powder. The graphene oxide (GO) can readily be suspended in polar medium. Figure 1 shows XRD spectra recorded before and after the oxidation of graphite powder. The peak seen at 26.5° in the graphite sample corresponds to the interspacing distance between the different graphene layers.[13] Chemical oxidation disrupts the ordering of

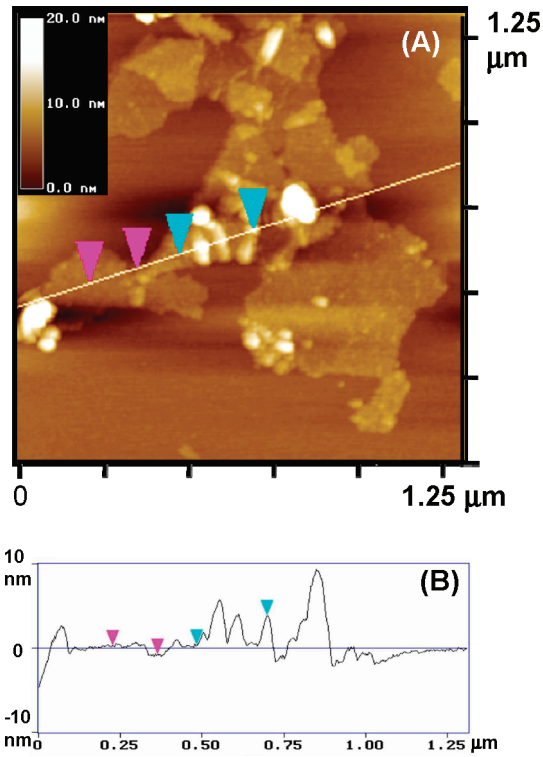

Figure 2. (A) AFM image of Pt deposited on graphene oxide following $NaBH_4$ reduction. (B) Cross section analysis of GO-Pt shows the graphene sheet height as 1.1 nm and the height of Pt nanoparticle as 3−5 nm. (X-axis units are in degrees.)

layers and causes the XRD peak to disappear and a smaller broader peak around 12° appears. As shown in earlier studies a variety of functional groups (epoxide, carboxyl, etc.) are introduced as the C−C bonds of the graphene sheet are broken during the oxidation process.[24,25] These functional groups assist in exfoliation of individual sheets, resulting in the loss of the ordered lattice structure in the sheets. If the graphene sheets stay ordered, the functional groups increase the interplanar distance between the sheets. This larger distance between graphene sheets shifts the XRD peak to smaller angles, thus explaining the broad peak near 12°. Other authors have seen similar trends in the shift of the XRD peak.[13]

GO-Pt Synthesis and Characterization. Szabo et al.[26] have shown that the surface charge of graphene is negative at pH 7 and can be modulated by varying pH of the medium. The negative charge of the graphene arises from the deprotonation of carboxylic acid groups and carries a zeta potential of −40 mV at pH 7. Details on the pzc (point of zero charge) and pH dependence of zeta potential of GO and chemically treated GO have been presented elsewhere.[27] Addition of acid (HCl) to a mixture of GO and H_2PtCl_6 neutralizes the negative charge of graphene oxide and facilitates binding of the $PtCl_6^{2-}$ ions. When $PtCl_6^{2-}$ is reduced by the addition of $NaBH_4$, the Pt particles stay attached to the graphene sheets. As shown earlier,[21] graphene sheets in fact act as a stabilizer for the gold nanoparticles formed using chemical reduction of $HAuCl_4$. The stability of the Pt particles obtained by the reduction of H_2PtCl_6 in graphene suspension at pH 2 was better than reduction carried out at pH 7.

Figure 2 A shows an AFM image of the partially reduced GO-Pt composite with graphene sheets and dispersed Pt nanoparticles. The height of a typical Pt particle anchored on 2-D carbon mat was measured to be 3−5 nm (Figure 2 B). This size is well within the optimal size range for electrocatalysts

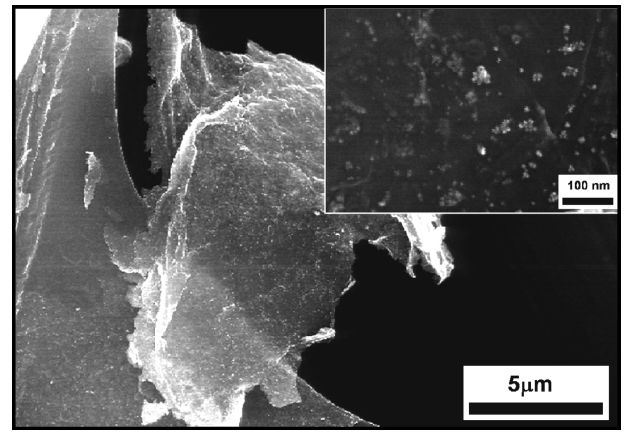

Figure 3. SEM image of GO-Pt deposited on carbon Toray paper. This image shows a few stacked graphene sheets laying across the carbon macrofiber of the Toray paper. The inset shows the magnified view of Pt nanoparticles dispersed on the graphene sheet.

used in fuel cell reactions.[23] The larger size peaks represent possible clustering of smaller size particles. The height of the graphene oxide sheet as measured from the cross section analysis was ∼1.1 nm and thus the image corresponds to a single sheet of graphene.[13,28] The ability to exfoliate graphite into single sheets provided a relatively large area on which to disperse the platinum particles.

The scanning electron micrograph (SEM) was recorded by depositing a partially reduced GO-Pt suspension onto a carbon Toray paper using a drop cast method. This allowed us to image the graphene sheets stuck between the carbon macro fibers of the Toray paper using SEM. Single sheets of graphene are usually difficult to image with good contrast using SEM. Stacked sheets, however, can readily be imaged using electron microscopy. The SEM picture in Figure 3 shows that the Pt particles are spread out on the graphene sheets. A magnified view in the inset shows fairly uniform distribution of Pt particles. A few aggregated clusters of Pt particles can also be seen in the magnified view of the graphene sheet. Pt particle aggregation is an important concern in the development of electrocatalyst film since it can significantly decrease the surface area.[28] Based on the SEM analysis, however, we consider such aggregation effects to be small. Electrochemical surface area measurements and fuel cell polarization curves were carried out to probe the effectiveness of Pt dispersion on the graphene sheets.

Electrochemically Active Surface Area (ECSA). The electrochemically active surface area (ECSA) provides important information regarding the number of available active sites. The ECSA accounts not only for the catalyst surface available for charge transfer but also includes the access of a conductive path to transfer the electrons to and from the electrode surface. Hydrogen adsorption/desorption in an electrochemical set up is commonly used to evaluate the ECSA. Figure 4 shows cyclic voltammograms of glassy carbon electrode coated with different electrocatalyst films that are in contact with 0.1 M H_2SO_4. At negative potentials (0 to −0.25 V vs SCE) the H^+ ions are reduced and the hydrogen atoms are absorbed. In the reverse scan the adsorbed hydrogen is desorbed resulting in the generation of anodic current. Integration of the area under the curve gives the amount of hydrogen desorbed, which in turn provides an estimate of the ECSA.

For the ECSA measurements the electrode was cycled between −0.25 and 0.9 V (vs SCE) in a nitrogen saturated 0.1 M H_2SO_4 solution at a rate of 20 mV/s until a stable hydrogen desorption peak was observed. The integrated area under the

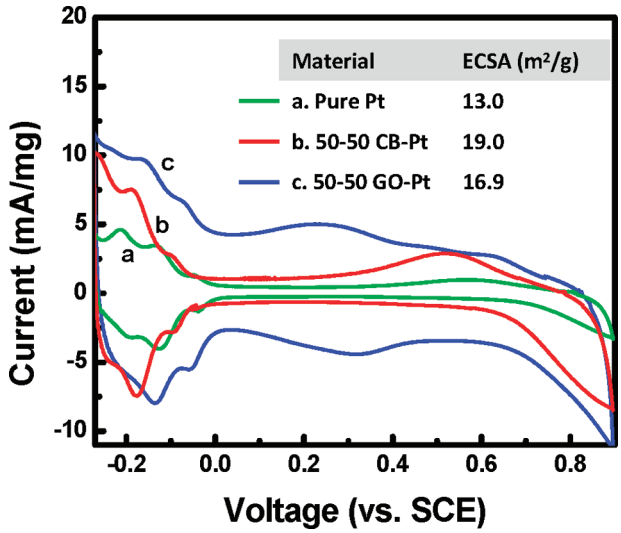

Figure 4. Cyclic voltammetry graphs of Pt, 50−50 (by weight) carbon black-Pt, and 50−50 (by weight) partially reduced graphene oxide-Pt. 20 μg/cm^2 of Pt was deposited on each electrode. 0.1 M H_2SO_4 was used as the electrolyte and the scan rate was 20 mV/s.

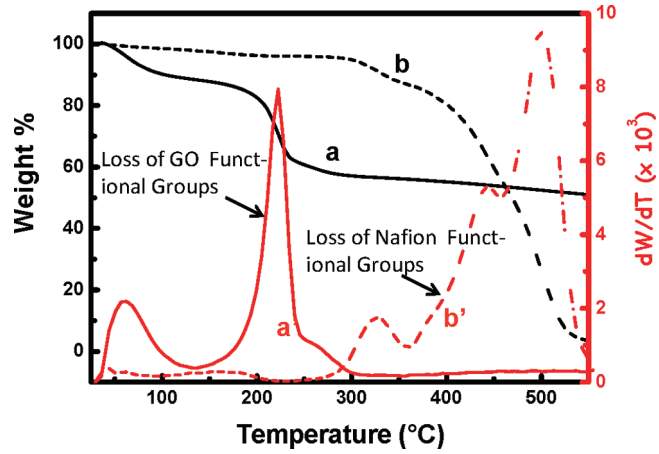

Figure 5. Thermogravimetric analysis of graphene oxide and Nafion ionomer. The black lines (a, b) show the change in weight while the red lines (a′,b′) show the derivative of the change in weight with respect to temperature. Both graphene oxide (a,a′) and Nafion (b,b′) lose water content before 100 °C. At 200 °C graphene oxide loses its functional groups and above 300 °C Nafion loses its functional groups.

desorption peak in the cyclic voltammogram represents the total charge relating to H^+ desorption, Q_H, and can be used to determine ECSA by employing eq 1.[29]

$$\mathrm{ECSA[cm^2Pt/gPt]} = \frac{\mathrm{charge}[Q_H, \mu\mathrm{C/cm^2}]}{210[\mu\mathrm{C/cm^2}] \times \mathrm{electrode\ loading[g\ Pt/cm^2]}} \quad (1)$$

The integrated area of cathodic and anodic current scans reflects the ECSA of individual electrocatalyst films. The carbon black supported Pt (CB-Pt) has higher ECSA than unsupported Pt, an observation that is in agreement with earlier published findings.[30] The dispersion of the Pt on a carbon support is expected to increase the available surface area for the electrocatalytic reaction. It is interesting to note that the partially reduced GO-Pt film exhibits ECSA higher than the unsupported Pt and the ECSA value (16.9 m^2/g) is close to the value of CB-Pt (19 m^2/g). Although GO is an insulator it undergoes partial reduction during the $NaBH_4$ treatment. A recent study has shown that the reduction of graphene oxide by $NaBH_4$ is nominally effective in improving the conductivity of the graphene films.[18]

Another reductant that is even more effective than $NaBH_4$ for reducing graphene oxide is hydrazine. The GO films reduced with hydrazine have been shown to achieve significantly higher conductivity than with other reductants.[16,18] The increase in conductivity is attributed to the increase in the sp^2 hybridization of the carbon network. The increase in sp^2 hybridization further allows π-π interaction between the individual graphene sheets, making the sheets agglomerate in suspension. Hence it is important to minimize the stacking of graphene sheets so that the effective area available for electrocatalyst is maximized. One possible approach to overcoming the stacking effect is to carry out the reduction in two steps. The first step is the partial reduction of graphene oxide with $NaBH_4$ along with Pt nanoparticle deposition. The deposition of the partially reduced GO-Pt on an electrode surface is then followed by the reduction of the film with hydrazine. The Pt particles anchored on individual graphene sheets help prevent their collapse and maximize the available electrocatalyst area.

When we attempted to carry out the two step reduction process of the graphene film additional problems were encountered. The partially reduced GO-Pt films cast on glassy carbon films upon exposure to an aqueous solution of hydrazine became physically unstable and sloughed off the glassy carbon electrode surface. Similar delamination of graphene films upon exposure to hydrazine was also reported by Becerril et al.[31] Any attempt to redisperse the delaminated film and deposit it on the glassy carbon electrode surface yielded poor quality films with lower ECSA. If one employed Toray carbon paper as the electrode substrate, however, the delamination problem is eliminated. The carbon fiber network of the Toray paper seems to provide better stability to the GO-Pt film. This method of casting electrocatalyst film on carbon fiber paper electrode is practical because of its direct use in preparing a membrane assembly for fuel cells. As mentioned in the experimental section, 10 μL of N_2H_4−H_2O was slowly drop cast across the Toray paper and dried in air (24 h). The films obtained by this procedure showed no visual evidence of delamination of the reduced GO-Pt films off the Toray paper.

The cyclic voltammogram of an air-dried, reduced GO-Pt film/carbon fiber electrode showed a large peak during the first oxidative scan corresponding to the oxidation of excess hydrazine adhering to the film. This peak decreased as we repeated the scan for 20 cycles. (See the Supporting Information.) The interference of excess hydrazine in the film could be minimized by heating the film at a higher temperature (300 °C). Improvement in the conductivity is usually seen when a graphene oxide film is heated after hydrazine deposition.[32] As shown earlier,[33] the higher temperature treatment is also effective in the removal of functional groups from the graphene oxide surface.

In order to probe the temperature effects we conducted thermogravimetric analysis (TGA) of graphene oxide and Nafion films. The TGA analysis shown in Figure 5 displays the weight loss of the samples (traces a and b in Figure 5) and the corresponding derivative of the weight loss with respect to temperature (traces a′ and b′ in Figure 5). The small derivative peaks seen at temperatures below 100 °C correspond to water loss in these two samples. Both graphene oxide[33] and Nafion[34] adsorb water under ambient conditions and readily desorb water upon heating. As the temperature is increased the GO functional groups are removed as is evidenced by the weight loss in the region of 150−300 °C. On the other hand, the Nafion ionomer remains unchanged at temperatures below 300 °C. Above 300

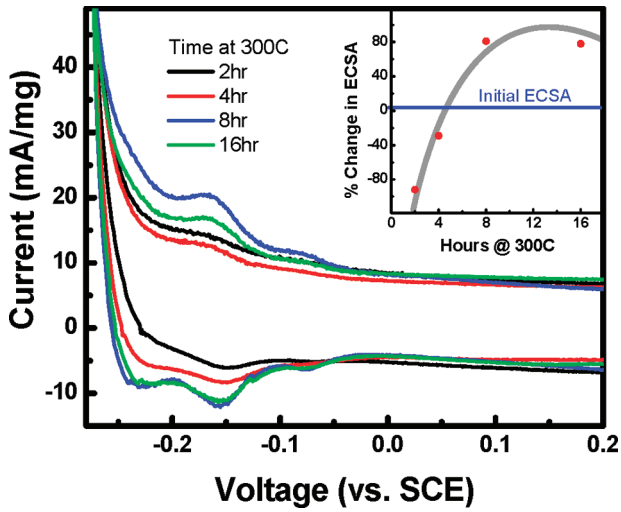

Figure 6. Cyclic voltammograms of hydrazine treated GO-Pt in 0.1 M H_2SO_4 and annealed at 300 °C for different periods of time (scan rate = 20 mV/s and catalyst concentration = 10 μg/cm^2 of Pt). Inset shows the relative increase of ECSA in these samples.

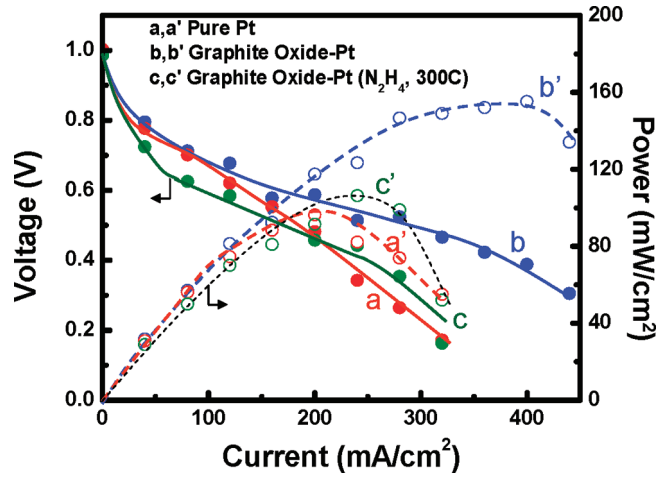

Figure 7. Galvanostatic fuel cell polarization (I−V) curves (a,b,c) and power characteristics (a′,b′,c′) of a fuel cell at 60 °C and 1 atm of back pressure. The cathode was composed of (a,a′) Pt, (b,b′) 1:1 GO-Pt, and 1:1 GO-Pt (hydrazine, 300 °C treated). Electrocatalyst concentration was maintained at 0.2 mg/cm^2 Pt. The anode for all experiments consisted of 0.5 mg/cm^2 Pt of E-Tek CB-Pt. The anode and cathode catalyst films were heat pressed on Nafion 115 membrane.

°C, the Nafion exhibits loss of weight due to polymer degradation and is fully degraded at 600 °C. These measurements provide an upper temperature limit for the treatment of graphene without losing the ionomer activity of Nafion. The temperature of 300 °C, thus, is a good high temperature treatment limit for removing leftover functional groups from graphene without affecting the ionomer properties of Nafion. This temperature limit is also low enough to retain the Pt particle size without the influence of high temperature ripening.[35]

After establishing the maximum treatment temperature as 300 °C we optimized the duration of the thermal treatment. Five Toray paper electrodes with GO-Pt electrocatalyst with a loading of ~10 μg/cm^2 of Pt were prepared. These electrodes were first analyzed for ECSA using cyclic voltammetry experiments in 0.1 M H_2SO_4. These electrodes exhibited an ECSA of ~11.5 m^2/g prior to heat treatment. The electrodes were then pretreated with hydrazine and annealed at 300 °C for different time intervals (2, 4, 8, and 16 h). The electrodes were again run through cyclic voltammetry experiments to compare the changes in ECSA and probe the effectiveness of the heat treatment. The comparison of the cyclic voltammograms and the relative change in ECSA are shown in Figure 6. The hydrogen desorption peaks for the 2-h heat treated sample showed a decrease, thus exhibiting a decrease in ECSA values as compared to its initial value. With increasing duration of heat treatment, however, the trend in ECSA reversed and we observed a net increase of about 80% following the 8 h treatment. The highest ECSA for the 8 h treated electrode was ~20 m^2/g. Further increase in the duration of the heat treatment did not show any significant change in ECSA. If the electrode was heated to 300 °C without hydrazine treatment we observed a decrease in ECSA of about 24%.

In addition to the drop cast method we also attempted to employ the electrophoretic deposition method[6] to cast the films of reduced GO-Pt films on Toray paper. This method was also effective in establishing good electrocatalytic activity. The electrode that was prepared by electrophoretic deposition of the reduced GO-Pt sample, pretreatment with hydrazine, and annealing at 300 °C for 8 h, gave about 77% increase in the ECSA (as compared to 80% achieved by drop cast method using similar treatment procedure. (See the Supporting Information.) These results further confirm that the increase in ECSA is independent of deposition method and is strongly dependent on the treatment following the deposition of the film. The results described here show that the importance of hydrazine treatment for reduction and reestablishment of sp^2 network of the graphene oxide. The higher temperature treatment is essential to remove the excess hydrazine from the catalyst surface.

Evaluation of Reduced GO-Pt Catalyst in Fuel Cell. Proton exchange membrane assemblies were constructed using different electrocatalysts deposited on Toray paper as the cathode and Pt-dispersed on carbon black (E-Tek CB-Pt) as the anode. The performances of these assemblies in a hydrogen fuel cell are compared in Figure 7. An unsupported Pt cathode was used as a reference to compare the performance of reduced graphene oxide supported Pt electrocatalysts. Both catalyst assemblies produced similar open-circuit voltage but the voltage drop varied as we drew the current from the cell. The partially reduced GO-Pt based fuel cell delivered a maximum power of 161 mW/cm^2 compared to 96 mW/cm^2 for an unsupported Pt based fuel cell. The dispersion of the electrocatalyst on graphene has been found to be useful for achieving relatively better performance in fuel cells.

Based on our ECSA results we expected a further increase in the fuel cell power output with the GO-Pt electrocatalyst films prepared following hydrazine and heat treatment. Instead the fuel cell showed a major drop in power output. We attributed this to the loss of proton conductivity property of the Nafion ionomer (used during the deposition of electrocatalyst) as it can undergo changes at higher temperature, thus causing an unintended drop in performance.[36]

This maiden effort to utilize graphene as a support material for the development of fuel cell electrocatalyst showed both the usefulness as well as the complexity of incorporating such composites in devices. Further work is necessary to develop strategies to improve the conductive properties of the graphene oxide so that the process is not detrimental to either the catalyst or the proton conductivity of the ionomer.

Acknowledgment. The research described herein was supported by the U.S. Army CECOM RDEC through Agreement DAAB07-03-3-K414. Such support does not constitute endorsement by the U.S. Army of the views expressed in this

publication. This is contribution No. NDRL 4786 from Notre Dame Radiation Laboratory.

Supporting Information Available: Details of hydrazine effects on the ECSA and ECSA results of electrophoretic deposition. This material is available free of charge via the Internet at http://pubs.acs.org.

References and Notes

(1) Costamagna, P.; Srinivasan, S. Quantum jumps in the PEMFC science and technology from the 1960s to the year 2000 Part I. Fundamental scientific aspects. *J. Power Source* **2001**, *102*, 242–252.

(2) Girishkumar, G.; Vinodgopal, K.; Kamat, P. V. Carbon nanostructures in portable fuel cells: Single-walled carbon nanotube electrodes for methanol oxidation and oxygen reduction. *J. Phys. Chem. B* **2004**, *108*, 19960–19966.

(3) Wang, C.; Waje, M.; Wang, X.; Tang, J. M.; Haddon, R. C.; Yan, Y. S. Proton exchange membrane fuel cells with carbon nanotube based electrodes. *Nano Lett.* **2004**, *4*, 345–348.

(4) Kim, C.; Kim, Y. J.; Kim, Y. A.; Yanagisawa, T.; Park, K. C.; Endo, M.; Dresselhaus, M. S. High performance of cup-stacked-type carbon nanotubes as a Pt-Ru catalyst support for fuel cell applications. *J. Appl. Phys.* **2004**, *96*, 5903–5905.

(5) Tang, H.; Chen, J. H.; Nie, L. H.; Liu, D. Y.; Deng, W.; Kuang, Y. F.; Yao, S. Z. High dispersion and electrocatalytic properties of platinum nanoparticles on graphitic carbon nanofibers (GCNFs). *J. Colloid Interface Sci.* **2004**, *269*, 26–31.

(6) Girishkumar, G.; Rettker, M.; Underhile, R.; Binz, D.; Vinodgopal, K.; McGinn, P.; Kamat, P. Single-wall carbon nanotube-based proton exchange membrane assembly for hydrogen fuel cells. *Langmuir* **2005**, *21*, 8487–8494.

(7) Lee, R. S.; Kim, H. J.; Fischer, J. E.; Thess, A.; Smalley, R. E. Conductivity enhancement in single-walled carbon nanotube bundles doped with K and Br. *Nature (London)* **1997**, *388*, 255–257.

(8) Seger, B.; K, A.; Vinodgopal, K.; Kamat, P. V. Platinum Dispersed on Silica Nanoparticles for PEM Fuel Cells. *J. Electroanal. Chem.* **2008**, *19*, 8–204.

(9) Meyers, J. P.; Darling, R. M. Model of carbon corrosion in PEM fuel cells. *J. Electrochem. Soc.* **2006**, *153*, A1432–A1442.

(10) Kongkanand, A.; Kuwabata, S.; Girishkumar, G.; Kamat, P. Single-wall carbon nanotubes supported platinum nanoparticles with improved electrocatalytic activity for oxygen reduction reaction. *Langmuir* **2006**, *22*, 2392–2396.

(11) Geim, A. K.; Novoselov, K. S. The rise of graphene. *Nat. Mater.* **2007**, *6*, 183–191.

(12) Novoselov, K. S.; Jiang, D.; Schedin, F.; Booth, T. J.; Khotkevich, V. V.; Morozov, S. V.; Geim, A. K. Two-dimensional atomic crystals. *Proc. Natl. Acad. Sci. (U.S.A.)* **2005**, *102*, 10451–10453.

(13) Schniepp, H. C.; Li, J. L.; McAllister, M. J.; Sai, H.; Herrera-Alonso, M.; Adamson, D. H.; Prud'homme, R. K.; Car, R.; Saville, D. A.; Aksay, I. A. Functionalized single graphene sheets derived from splitting graphite oxide. *J. Phys. Chem. B* **2006**, *110*, 8535–8539.

(14) Brodie, B. Sur le poids atomique du graphite. *Ann. Chim. Phys.* **1860**, *59*, 7.

(15) Hummers, W. S.; Offeman, R. E. Preperation of Graphitic Oxide. *J. Am. Chem. Soc.* **1958**, *80*, 1339–1339.

(16) Stankovich, S.; Dikin, D. A.; Piner, R. D.; Kohlhaas, K. A.; Kleinhammes, A.; Jia, Y.; Wu, Y.; Nguyen, S. T.; Ruoff, R. S. Synthesis of graphene-based nanosheets via chemical reduction of exfoliated graphite oxide. *Carbon* **2007**, *45*, 1558–1565.

(17) Bourlinos, A. B.; Gournis, D.; Petridis, D.; Szabo, T.; Szeri, A.; Dekany, I. Graphite oxide: Chemical reduction to graphite and surface modification with primary aliphatic amines and amino acids. *Langmuir* **2003**, *19*, 6050–6055.

(18) Si, Y.; Samulski, E. T. Synthesis of Water Soluble Graphene. *Nano Lett.* **2008**, *8*, 1679–1682.

(19) Williams, G.; Seger, B.; Kamat, P. V. TiO_2-graphene nanocomposites. UV-assisted photocatalytic reduction of graphene oxide. *ACS Nano* **2008**, *2*, 1487–1491.

(20) Cassagneau, T.; Fendler, J. H. Preparation and layer-by-layer self-assembly of silver nanoparticles capped by graphite oxide nanosheets. *J. Phys. Chem. B* **1999**, *103*, 1789–1793.

(21) Muszynski, R.; Seger, B.; Kamat, P. V. Decorating Graphene Sheets with Gold Nanoparticles. *J. Phys. Chem. C* **2008**, *112*, 5263–5266.

(22) Kamat, P. V.; Thomas, K. G.; Barazzouk, S.; Girishkumar, G.; Vinodgopal, K.; Meisel, D. Self-assembled linear bundles of single wall carbon nanotubes and their alignment and deposition as a film in a dc field. *J. Am. Chem. Soc.* **2004**, *126*, 10757–10762.

(23) Vielstich, W.; Lamm, A.; Gasteiger, H. A. *Handbook of Fuel Cells: Fundamentals, Technology, and Applications*; John Wiley & Sons: New York, 2003; Vol. 3.

(24) Lerf, A.; He, H. Y.; Forster, M.; Klinowski, J. Structure of graphite oxide revisited. *J. Phys. Chem. B* **1998**, *102*, 4477–4482.

(25) He, H. Y.; Klinowski, J.; Forster, M.; Lerf, A. A new structural model for graphite oxide. *Chem. Phys. Lett.* **1998**, *287*, 53–56.

(26) Szabo, T.; Tombacz, E.; Illes, E.; Dekany, I. Enhanced acidity and pH-dependent surface charge characterization of successively oxidized graphite oxides. *Carbon* **2006**, *44*, 537–545.

(27) Li, D.; Muller, M. B.; Gilje, S.; Kaner, R. B.; Wallace, G. G. Processable aqueous dispersions of graphene nanosheets. *Nat. Nanotechnol.* **2008**, *3*, 101–105.

(28) Stankovich, S.; Piner, R. D.; Chen, X. Q.; Wu, N. Q.; Nguyen, S. T.; Ruoff, R. S. Stable aqueous dispersions of graphitic nanoplatelets via the reduction of exfoliated graphite oxide in the presence of poly(sodium 4-styrenesulfonate). *J. Mater. Chem.* **2006**, *16*, 155–158.

(29) Sogaard, M.; Odgaard, M.; Skou, E. M. An improved method for the determination of the electrochemical active area of porous composite platinum electrodes. *Solid State Ionics* **2001**, *145*, 31–35.

(30) Ticianelli, E. A.; Derouin, C. R.; Srinivasan, S. Localization of Platinum in Low Catalyst Loading Electrodes to Attain High-Power Densitieis in SPE Fuel-Cells. *J. Electroanal. Chem.* **1988**, *251*, 275–295.

(31) Becerril, H. A.; Mao, J.; Liu, Z.; Stoltenberg, R. M.; Bao, Z.; Chen, Y. Evaluation of solution-processed reduced graphene oxide films as transparent conductors. *ACS Nano* **2008**, *2*, 463–470.

(32) Szabo, T.; Szeri, A.; Dekany, I. Composite graphitic nanolayers prepared by self-assembly between finely dispersed graphite oxide and a cationic polymer. *Carbon* **2005**, *43*, 87–94.

(33) Niyogi, S.; Bekyarova, E.; Itkis, M. E.; McWilliams, J. L.; Hamon, M. A.; Haddon, R. C. Solution properties of graphite and graphene. *J. Am. Chem. Soc.* **2006**, *128*, 7720–7721.

(34) Zawodzinski, T. A.; Derouin, C.; Radzinski, S.; Sherman, R. J.; Smith, V. T.; Springer, T. E.; Gottesfeld, S. Water-Uptake by and Transport Through Nafion(R) 117 Membranes. *J. Electrochem. Soc.* **1993**, *140*, 1041–1047.

(35) Bett, J. A.; Kinoshit, K.; Stonehar, P. Crystallite Growth of Platinum Dispersed on Graphitized Carbon-Black. *J. Catal.* **1974**, *35*, 307–316.

(36) Deng, Q.; Wilkie, C. A.; Moore, R. B.; Mauritz, K. A. TGA-FTi.r. investigation of the thermal degradation of Nafion (R) and Nafion (R)/[silicon oxide]-based nanocomposites. *Polymer* **1998**, *39*, 5961–5972.

JP900360K